Proc. Natl. Acad. Sci. USA
Vol. 85, pp. 9317–9321, December 1988
Microbiology

Characterization of invasion plasmid antigen genes (*ipaBCD*) from *Shigella flexneri*

(epithelial cell entry/bacterial virulence/hydrophilicity/regulon)

MALABI M. VENKATESAN, JERRY M. BUYSSE, AND DENNIS J. KOPECKO

Division of Communicable Diseases and Immunology, Walter Reed Army Institute of Research, Washington, DC 20307-5100

Communicated by David D. Sabatini, July 7, 1988 (received for review April 28, 1988)

ABSTRACT **The large invasion plasmid of *Shigella flexneri* M9OT-W was used to generate recombinant plasmids carrying the *ipaA*, *-B*, *-C*, and *-D* genes, whose products are associated with the entry of the bacteria into colonic epithelial cells. Complete DNA sequences of *ipaB*, *-C*, and *-D* were determined. The proteins predicted (62, 42, and 37 kDa, respectively) from the nucleotide sequences lack a signal-peptide sequence. Hydrophilic segments of the IpaB and IpaC proteins were found to overlap known epitopic domains of these membrane antigens. Analysis of total RNA demonstrated that temperature control of *ipa* gene expression occurs at the level of transcription. Multiple mRNA bands were detected by using *ipa* gene fragments as hybridization probes, and a putative transcript map for the *ipa* genes was constructed. Comparison of this map with the DNA sequence reveals a complex system of *ipa* gene regulation.**

The invasion of human colonic epithelial cells by *Shigella* and enteroinvasive *Escherichia coli* (EIEC) triggers a series of host–parasite interactions resulting in the syndrome known as bacillary dysentery. Genetic studies established that the ability to invade epithelial cells is encoded by a 210-kilobase (kb) plasmid, commonly referred to as the invasion plasmid, that is present in all virulent *Shigella* and EIEC strains (for recent reviews, see refs. 1 and 2). Although complete virulence requires chromosomal genes, the transfer of the invasion plasmid from *Shigella* to an *E. coli* K-12 strain has demonstrated that the plasmid is sufficient to promote epithelial cell entry. The invasion plasmid controls the synthesis of several unique polypeptides. Sodium dodecyl sulfate (SDS) lysates of plasmid-containing invasive *Shigella* strains, when reacted with human or monkey immune serum on Western blots, consistently demonstrate the presence of 140-kDa, 78-kDa (invasion plasmid antigen A, IpaA), 62-kDa (IpaB), 42-kDa (IpaC), and 37-kDa (IpaD) proteins (3). Although these antigens are minor components of total bacterial proteins, they are responsible for the major humoral response in an infected host (3). Synthesis of these immunogens is repressed at 30°C and restored at 37°C, an observation that parallels the loss and gain, respectively, of the bacterial invasive phenotype (4). Monoclonal antibodies to the IpaB and IpaC proteins, reacted in whole-cell ELISAs with virulent *Shigella*, strongly indicate that these proteins are localized on the bacterial membrane surface (5).

In vitro studies with cultured epithelial cells (HeLa, BHK, etc.) established that a 37-kb DNA segment from the invasion plasmid of *S. flexneri* is sufficient to restore the invasive phenotype to a plasmid-cured *Shigella* strain (4). Tn*5* mutagenesis defined several regions within this 37-kb fragment that are necessary for this function (4, 6, 7). The *ipaBCDA* genes represent one of these regions (6–8); hybridization studies showed that these genes are highly conserved in all *Shigella* and EIEC strains and are not homologous to DNA from other enteric or nonenteric bacteria (9).

We report here the DNA sequence of the *ipaB*, *-C*, and *-D* genes as well as two adjacent genes.* We provide data to support the hypothesis that these genes comprise multiple units of transcription. Finally, the regulation of *ipa* gene expression by temperature is shown to occur at the level of mRNA synthesis.

MATERIALS AND METHODS

Bacterial Strains and Plasmids. Bacterial strains and plasmids used in this study have been described (8, 9).

Construction of Recombinant Plasmids. *Hin*dIII- or *Eco*RI-digested invasion plasmid DNA cloned into pBR322 was used to generate pHC17 and pEC14, respectively. pEC15 was derived from pEC14 by cloning the 3.5-kb *Eco*RI–*Bam*HI fragment into pUC18.

Minicell Analysis of Recombinant Plasmids. pHC17, pEC14, and pBR322 were transformed into the *E. coli* minicell strain DS410. Minicells were isolated and labeled with [^{35}S]methionine (5 mCi; specific activity, 600 Ci/mmol; Amersham; 1 Ci = 37 GBq) essentially as described (10).

Northern Blot Hybridization. Total RNA was prepared from M9OT-W and M9OT-A3 grown at 30°C or 37°C. Cells grown to an OD_{600} of 0.8 were treated with lysozyme (2 mg/ml) in 25% sucrose/50 mM Tris·HCl, pH 7.5, and incubated at 0°C for 10 min to obtain spheroplasts. RNA was then isolated by extraction with 6 M guanidine thiocyanate and centrifugation through a CsCl gradient (11). *ipa* gene fragments were nick-translated with [α-^{32}P]dCTP and used as probes under stringent hybridization conditions (8, 9).

DNA Sequencing. The 4.7-kb *Hin*dIII insert DNA from pHC17 as well as a series of *ipa* gene-containing fragments from λgt11 *ipa* clones were ligated into pUC18 for double-stranded DNA sequencing (Fig. 1). A 5.2-kb region was thus completely sequenced in both directions by the dideoxy chain-termination reaction (12) using the Sequenase-based DNA sequencing kit from United States Biochemical, Cleveland. Oligonucleotide primers were synthesized on a model 8600 DNA synthesizer (Biosearch, San Rafael, CA).

Sequence Analysis. The MacGene Plus application (Macintosh) was used on a Macintosh SE microcomputer to search for reading frames and restriction sites, derive protein sequences from nucleic acid data, and predict protein secondary structures. Regions of dyad symmetry were identified by the DNASEQ program run by the computer facilities of the National Institutes of Health, Bethesda, MD.

The publication costs of this article were defrayed in part by page charge payment. This article must therefore be hereby marked "*advertisement*" in accordance with 18 U.S.C. §1734 solely to indicate this fact.

Abbreviation: EIEC, enteroinvasive *Escherichia coli*.

*The sequence reported in this paper is being deposited in the EMBL/GenBank data base (IntelliGenetics, Mountain View, CA, and Eur. Mol. Biol. Lab., Heidelberg) (accession no. J04117).

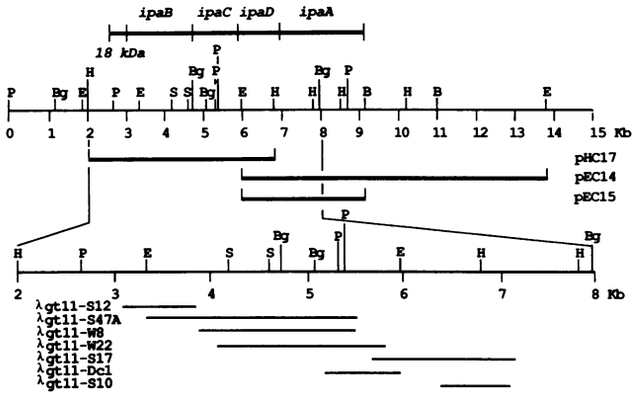

FIG. 1. Genetic map and sequencing strategy of *ipa* genes. The thin bar represents 15 kb of DNA of the invasion plasmid pWR100 showing the organization and a partial restriction endonuclease map of the *ipaBCDA* genes and the gene encoding the 18-kDa peptide. DNA fragments cloned in pHC17, pEC14, and pEC15 are shown as solid bars. The *Hin*dIII–*Bgl* II fragment delineates the boundaries of the DNA sequenced and is magnified to show the fragments in λgt11 clones that were used to generate pUC18 recombinants for sequence analysis and for hybridization probes. B, *Bgl* II; E, *Eco*RI; H, *Hin*dIII; S, *Sal* I; P, *Pst* I.

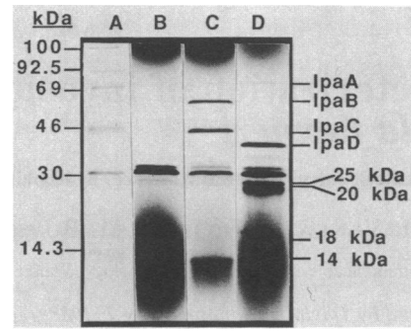

FIG. 2. Minicell analysis of pHC17 and pEC14. *E. coli* DS410 minicells carrying pHC17 (lane C), pEC14 (lane D), or pBR322 (lane B) were labeled with [^{35}S]methionine and lysed in SDS buffer. Labeled proteins (10^6 cpm per lane) were separated by discontinuous SDS/20% PAGE and visualized by autoradiography. The sizes of [^{14}C]protein standards (lane A) are indicated at left and the sizes of the proteins synthesized by the transformants are indicated at right.

RESULTS

Characterization of Recombinant Plasmids. pHC17 and pEC14 were constructed to obtain suitable templates for both DNA sequencing and expression of Ipa proteins. Fig. 1 indicates the location of their inserts relative to the *ipa* gene map (8). IpaB and IpaC monoclonal antibodies (5), as well as immune sera from infected monkeys, reacted strongly with the 62-kDa (IpaB) and 42-kDa (IpaC) antigens produced by HB101(pHC17) (data not shown). HB101(pEC14) and HB101(pEC15) synthesized 78-kDa (IpaA) and 37-kDa (IpaD) proteins as detected by monkey and human polyclonal sera. This last observation sets the rightward boundary for the *ipaA* gene as shown in Fig. 1. Whole-cell ELISAs with monoclonal antibodies showed that the IpaB and IpaC proteins synthesized from HB101(pHC17) were not surface-expressed (unpublished observation). In addition, the two recombinant clones are noninvasive in HeLa cell invasion assays (1, 2).

To identify all of the gene products encoded by pHC17 and pEC14, *in vivo* expression was monitored in the *E. coli* minicell strain DS410 (Fig. 2). In addition to the IpaB and IpaC proteins, DS410(pHC17) demonstrated the synthesis of two smaller peptides of 14 and 18 kDa. The 18-kDa peptide band represented a minor component on these gels. Similarly, DS410(pEC14) synthesized IpaA and IpaD as well as two prominent smaller peptides of 20 and 25 kDa. The Ipa proteins, synthesized in minicells, reacted on Western blots with immune sera from rabbits; the 14-, 18-, 20-, and 25-kDa proteins, however, did not react with the immune sera (data not shown). Since pEC15 (Fig. 1) encodes complete IpaA and IpaD proteins, we believe that the two smaller peptides seen in DS410(pEC14) are encoded distal to the *Bam*HI site at the rightward boundary of *ipaA* (Fig. 1).

Northern Blot Analysis of *ipa* Genes. Hybridization with *ipa* probes detected several bands in RNA prepared from M9OT-W cells grown at 37°C but not in RNA from cells grown at 30°C (Fig. 3*A*, lanes a and b). As expected, RNA from M9OT-A3, which has deleted a 30- to 40-kb region of the invasion plasmid including the *ipaBCDA* genes (9), grown at either temperature did not hybridize to any of the *ipa* probes (Fig. 3*B*, lanes a and c). The 4.7-kb *Hin*dIII insert fragment of pHC17 hybridized predominantly to two RNA bands corresponding to 2.4 and 1.4 kb (Fig. 3*A*, lane 1a). The *ipaB* probe (λgt11-S12; Fig. 1) hybridized mainly with the 2.4-kb transcript, whereas the *ipaC* probe (λgt11-W22; Fig. 1)

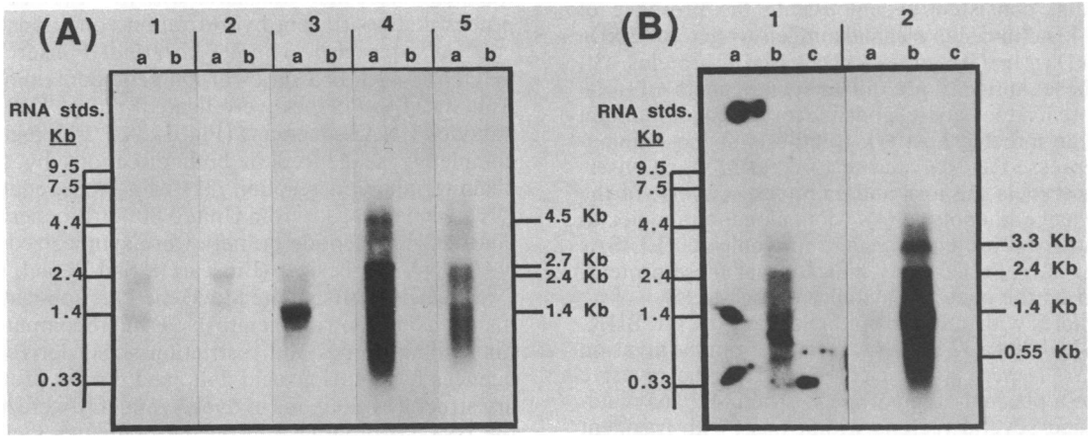

FIG. 3. Northern blot analysis of RNA hybridized to *ipa* genes. Total RNA (20 μg per lane) was electrophoresed in 1% agarose/2.2 M formaldehyde gels and transferred to nitrocellulose. Individual lanes were cut out and hybridized to *ipa* gene segments. (*A*) RNA from M9OT-W grown at 37°C (lanes a) or 30°C (lanes b) was probed with *ipa* DNA from pHC17 (lanes 1), S12 (lanes 2), W22 (lanes 3), S10 (lanes 4), or PEC15 (lanes 5). (*B*) RNA from M9OT-A3 grown at 37°C (lanes a) or from M9OT-W grown at 37°C (lanes b) or 30°C (lanes c) was hybridized to *ipa* gene segments from S12 (lanes 1) and W22 (lanes 2). Autoradiographs in *B* were exposed for 72 hr. Sizes of RNA standards (Bethesda Research Laboratories) and transcripts are indicated at left and right, respectively.

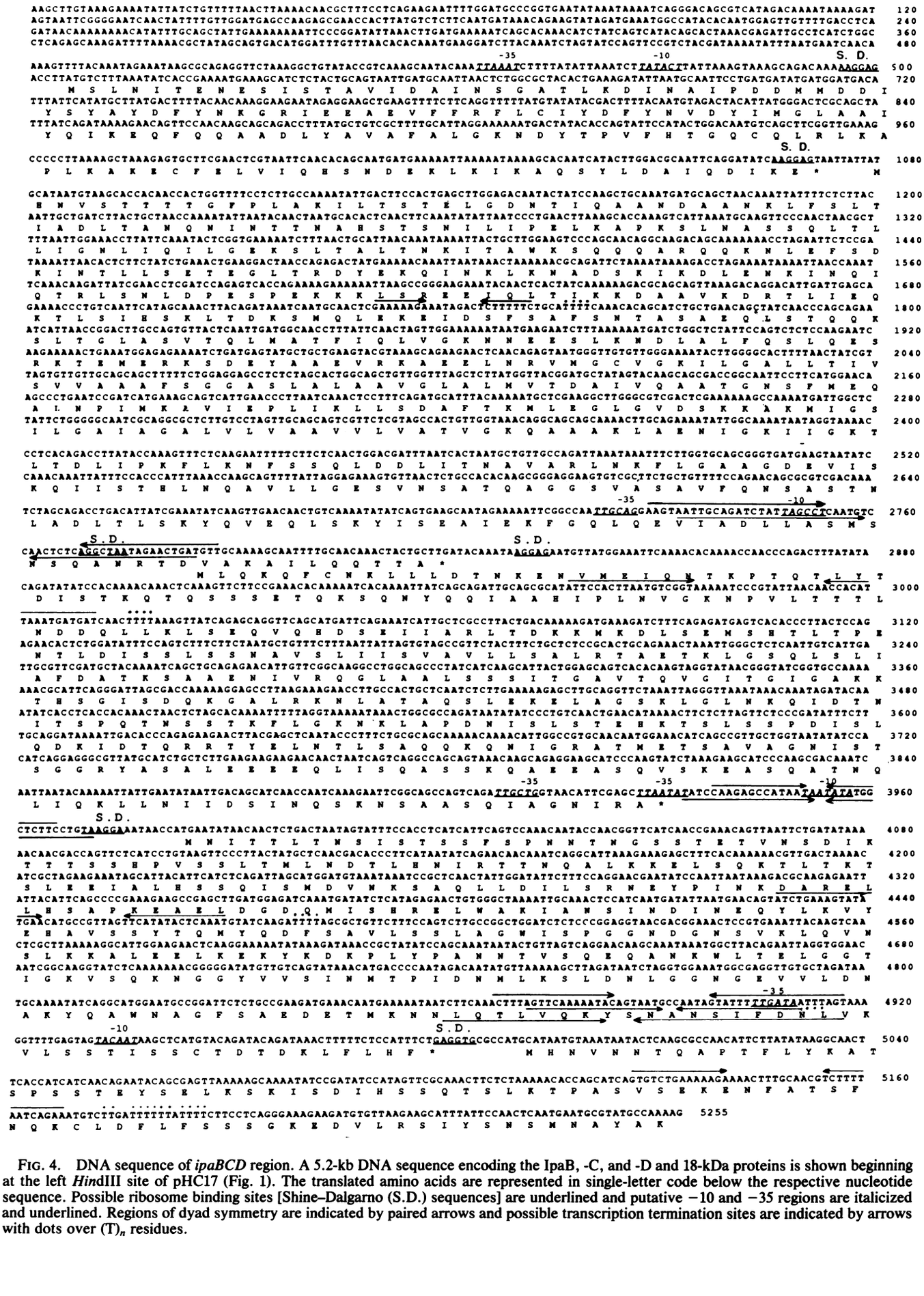

FIG. 4. DNA sequence of *ipaBCD* region. A 5.2-kb DNA sequence encoding the IpaB, -C, and -D and 18-kDa proteins is shown beginning at the left *Hin*dIII site of pHC17 (Fig. 1). The translated amino acids are represented in single-letter code below the respective nucleotide sequence. Possible ribosome binding sites [Shine–Dalgarno (S.D.) sequences] are underlined and putative −10 and −35 regions are italicized and underlined. Regions of dyad symmetry are indicated by paired arrows and possible transcription termination sites are indicated by arrows with dots over $(T)_n$ residues.

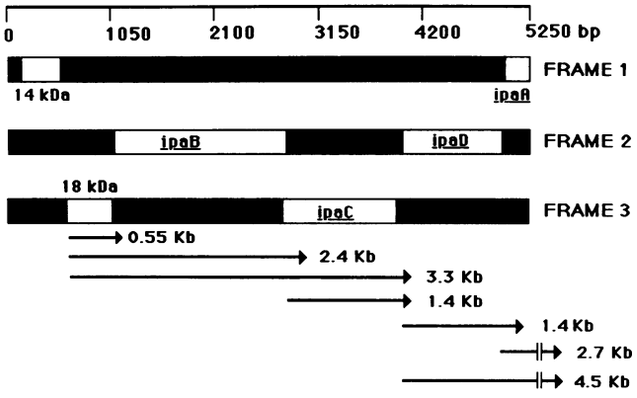

FIG. 5. Schematic representation of *ipaBCD* sequence and RNA transcripts. The open reading frames from Fig. 4 are presented as open boxes. The transcripts (arrows) detected by hybridization with individual *ipa* fragments are mapped onto this sequence and shown below the protein-coding regions. Transcript lengths are indicated in kb. Scale at top is in base pairs (bp).

reacted predominantly with the 1.4-kb RNA (Fig. 3*A*, lanes 2a and 3a). Longer exposure (72 hr) of the *ipaB*-probed RNA filter revealed two additional bands at 3.3 and 0.5 kb (Fig. 3*B*, lane 1b). The 3.3- and 2.4-kb transcripts were also seen on longer exposure of the filter hybridized to the *ipaC* probe (Fig. 3*B*, lane 2b). DNA fragments corresponding to *ipaDA* (pEC15) and *ipaD* (λgt11-S10, Fig. 1) hybridized to a unique set of transcripts of 4.5, 2.7, and 1.4 kb (Fig. 3*A*, lanes 4a and 5a); the 4.5-kb RNA was detected more easily with the *ipaDA* segment of pEC15.

Sequence Analysis of *ipaBCD*. The DNA sequences of the *ipaBCD* genes along with their predicted amino acid sequences are presented in Fig. 4 and schematically represented in Fig. 5. The locations of the open reading frames are consistent with the previously determined positions of the *ipaB*, *-C*, *-D*, and *-A* genes (8). The sizes of the proteins (62, 42, and 37 kDa for IpaB, -C, and -D) calculated from the sequences agree well with those estimated from SDS/PAGE (3, 8). Two smaller peptides (18 and 14 kDa) are also predicted by the nucleotide sequence (Figs. 4 and 5), which could account for the observed smaller peptides synthesized in DS410(pHC17) (Fig. 2).

The translational initiation codons for *ipaBCD* as well as the 18-kDa peptide are preceded by good ribosome binding sites (Shine–Dalgarno sites, S.D. in Fig. 4) 6–9 bp upstream of the respective ATG codons. *ipaB* initiates at bp 1079 and terminates at bp 2818 (Fig. 4). The 5′ end of *ipaC* contains two potential initiation codons (at bp 2769 and 2830), the second of which is preceded by a Shine–Dalgarno sequence closer to the consensus than the first (AGGCT vs. AGGAG; Fig. 4). A potential overlap of 34 bp between *ipaB* and *ipaC* would be eliminated if translation were to initiate at the second ATG codon. However, the size of the protein predicted by the use of the second initiation codon would be slightly smaller (37 kDa) than that estimated from SDS/PAGE or predicted by the use of the first ATG triplet (42 kDa). *ipaD* begins at bp 3983 and terminates at bp 4978 (Fig. 4). An open reading frame at the end of *ipaD* and the appearance of a ribosome binding site at bp 4980 (Fig. 4) determine what we believe to be the genetic location of the 5′ end of *ipaA* as indicated in Fig. 1. The 18-kDa protein begins at bp 606 and terminates at bp 1070. The absence of a suitable Shine–Dalgarno sequence upstream of bp 151, which opens the reading frame for a 14-kDa peptide, leaves the possibility that this site may not be used *in vivo*.

Significant regions of dyad symmetry occur throughout the body of the DNA sequence. Interestingly, several of these were found to overlap in areas that provided a junction between the termination of one Ipa protein and the beginning of another (Fig. 4). Some dyad symmetries seen embedded within the coding sequences of the *ipa* genes display characteristics of transcription termination structures, as shown in Fig. 4 and discussed below. The −10 (TANNNT) and −35 (TTGACA) sequences found in *E. coli* promoters (13) are indicated in front of the sequence encoding the 18-kDa peptide but not in front of *ipaB* (Fig. 4), suggesting that perhaps the two genes share common RNA polymerase binding sites. A region of hyphenated dyad symmetry followed by $(T)_n$ residues, indicated near bp 3000 and 4500 (Fig. 4) could act as potential transcription termination sites for *ipaB* and *ipaC* and, in concert with their transcription initiation sites, could account for the 2.4- and 1.4-kb *ipaB*- and *ipaC*-specific mRNA bands (Fig. 3 and Fig. 5). RNA polymerase binding sites are also indicated in front of *ipaD* (Fig. 4), which along with a transcription termination-like structure near bp 5160 could account for the 1.4-kb transcript seen with *ipaD*-probed RNA (Fig. 3*A*). Based on the sizes of the RNAs detected with discrete *ipa* gene probes (Fig. 3) and the putative transcriptional signals in the DNA sequence (Fig. 4), we have projected a tentative transcript map onto the genetic map of the *ipa* region (Fig. 5).

Secondary Structure of IpaBCD Proteins. The hydrophilicity profiles of the IpaB, -C, and -D proteins deduced from the DNA sequence indicate that all three proteins have a pronounced hydrophilic structure (Fig. 6). A hydrophobic stretch of amino acids with the characteristics of a signal-peptide sequence (15) was not seen in any of the three Ipa proteins. Monoclonal antibodies to IpaB and IpaC have been used to define several epitopes of these two proteins (8). Superimposition of the epitopic map onto the hydropathy profile shows that the antigenic regions of IpaB and IpaC coincide with hydrophilic regions (Fig. 6).

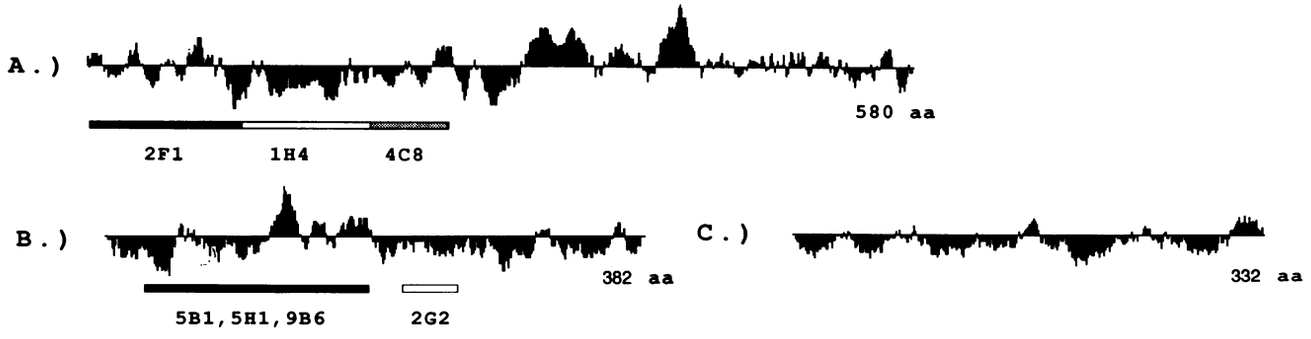

FIG. 6. Hydrophilicity profiles (14) of IpaB (*A*), IpaC (*B*), and IpaD (*C*). Positive hydrophilicity is indicated by areas shown as inverted peaks. Bars below the profiles reflect the epitopic domains recognized by individual monoclonal antibodies to IpaB (2F1, 1H4, and 4C8) or IpaC (5B1, 5H1, 9B6, and 2G2; ref. 5). aa, Amino acids.

DISCUSSION

Entry of colonic epithelial cells by *Shigella* requires an endocytic event, in a manner analogous to the engulfment of particles by professional phagocytes (16). The Ipa proteins, located in the bacterial membrane, may play a role in triggering the endocytic process. Subsequent to infection of the epithelial cell, a plasmid-mediated hemolytic activity is implicated in the escape of the pathogen from the endocytic vacuole, an event that correlates with the ability of *Shigella* to multiply and disseminate intracellularly (17). One or more of the Ipa proteins may also be involved in this activity. The distribution of epitopic domains in IpaB and IpaC reinforces the prediction that many antigenic determinants correlate with local upspikes in the protein hydrophilicity profile (18). It appears likely that the presence of the Ipa proteins on the bacterial cell surface, as measured in whole-cell ELISAs (5), is a prerequisite for their role in invasion. Cosmid clones of the invasion plasmid that synthesize all four of the Ipa proteins but do not present the antigens on the surface are also noninvasive (unpublished observation). The absence of a signal sequence, which in other Gram-negative bacteria serves to direct outer membrane proteins onto the cell surface (19), suggests that additional factors may be necessary for Ipa protein positioning in the *Shigella* membrane. An analogous situation is seen with the expression of the hemolysins, bacteriocins, and the K88ab fimbrial subunits of *E. coli* (20–22), each of which requires specific helper proteins for translocation across the cell envelope. Epithelial cell entry by *Shigella* involves several unique proteins and thus contrasts with the invasion system of *Yersinia enterocolitica*, where a single 100-kDa outer membrane protein is sufficient to render *E. coli* K-12 invasive (23).

Temperature regulation of virulence-associated genes appears to be common among pathogenic bacteria. Along with the Ipa proteins of *Shigella*, the adhesion antigens of *Salmonella typhimurium* (24) and *E. coli* (25), the K1 capsular antigen of *E. coli* (26), and the virulence-related low-calcium response of *Yersinia* (27, 28) are temperature-regulated. Thermal regulation in these instances occurs at the level of transcription, as seen with the *Shigella* Ipa antigens, and usually affects the expression of structural genes for outer membrane proteins. Since protein translocation across membranes is an energy-dependent process (29), the temperature regulation of virulence-related outer membrane proteins could reflect an adaptation to conserve energy until a suitable niche for rapid growth is presented to the bacterial cell. Recently, a chromosomal gene (*virR*) has been found to encode a trans-acting repressor that regulates the expression of *Shigella* virulence and the expression of the *ipa* genes in response to temperature (30). Presumably this repressor acts directly on the transcription of the *ipa* genes or through a positive activator of *ipa* gene expression. We have recently obtained evidence that certain Tn*5* insertion mutations in the 37-kb invasive fragment that repress the synthesis of all four *ipa* genes can be complemented by pEC14 to restore synthesis as well as the invasive phenotype (unpublished data). Complementation is not restored by pEC15. These results indicate the presence of a trans-acting positive effector on pEC14 that maps to the right of *ipaA*. This idea is supported by the incomplete homologies with the consensus −35 sequence that are observed in the 18-kDa protein gene and in the *ipaC*, *-D*, and *-A* genes, a feature commonly found in positively activated promoter sequences (13).

The presence of multiple discrete transcripts specific for individual *ipa* gene probes, as well as our earlier observation with λgt11 clones that expressed independent Ipa proteins (8), suggests that these genes are regulated as a group of operons (a regulon). Although some Tn*5* insertion mutants can simultaneously alter the expression of all four Ipa proteins, a property expected if the proteins are clustered in a single operon, the continued expression of IpaC in these mutants has been attributed to either a better ribosome binding site or the presence of a secondary promoter at the beginning of the *ipaC* gene (6). Regulation of the *ipa* genes as a regulon by common repressor and activator molecules would also be consistent with the observations made with these Tn*5* mutants. A similar model of gene regulation is found in the low-calcium response of *Y. pestis* (27), which is mediated by a locus (*lcrF*) that regulates transcription from two widely separated loci.

It is possible that individual *ipa* transcripts are derived from processing of larger transcripts as reported recently for pilin gene expression in *E. coli* (31). For example, the 2.4- and 1.4-kb RNA bands seen with individual *ipaB* and *ipaC* probes could conceivably be derived from the 3.3-kb transcript by an unknown processing scheme. The presence of extensive stem–loop structures at the transition of the *ipa* gene coding sequences, seemingly sequestering both ribosome and RNA polymerase recognition sites (Fig. 4), points to a role for these structures in transcription initiation/termination, translation, or RNA processing.

We are grateful to Jonathan Mills, Barry Cohen, and Ken Stover (Walter Reed Army Institute of Research) and S. Venkatesan (National Institute of Allergy and Infectious Diseases) for help and advice.

1. Kopecko, D. J., Venkatesan, M. & Buysse, J. M. (1988) in *Enteric Infection: Mechanism, Manifestations and Management*, eds. Keusch, G. & Farthing, M. (Chapman & Hall, London), pp. 41–64.
2. Hale, T. L. & Formal, S. B. (1986) *Microb. Pathog.* **1**, 511–518.
3. Oaks, E. V., Hale, T. L. & Formal, S. B. (1986) *Infect. Immun.* **53**, 57–63.
4. Maurelli, A. T., Baudry, B., DeHauteville, H., Hale, T. L. & Sansonetti, P. J. (1985) *Infect. Immun.* **49**, 164–171.
5. Mills, J. A., Buysse, J. M. & Oaks, E. V. (1988) *Infect. Immun.* **56**, 2933–2941.
6. Baudry, B., Maurelli, A. T., Clerc, P., Sadoff, J. & Sansonetti, P. J. (1987) *J. Gen. Microbiol.* **133**, 3403–3413.
7. Sasakawa, C., Kamata, K., Sakai, T., Makino, S., Yamada, M., Okada, N. & Yoshikawa, M. (1988) *J. Bacteriol.* **170**, 2480–2484.
8. Buysse, J. M., Stover, C. K., Oaks, E. V., Venkatesan, M. & Kopecko, D. J. (1987) *J. Bacteriol.* **169**, 2561–2569.
9. Venkatesan, M., Buysse, J. M. & Kopecko, D. J. (1988) *J. Clin. Microbiol.* **26**, 261–266.
10. Newland, J. W., Green, B. A., Foulds, J. & Holmes, R. K. (1985) *Infect. Immun.* **47**, 691–696.
11. Maniatis, T., Fritsch, E. F. & Sambrook, J. (1982) *Molecular Cloning: A Laboratory Manual* (Cold Spring Harbor Lab., Cold Spring Harbor, NY).
12. Sanger, F., Nicklen, S. & Coulson, A. R. (1977) *Proc. Natl. Acad. Sci. USA* **74**, 5463–5467.
13. McClure, W. R. (1985) *Annu. Rev. Biochem.* **54**, 171–204.
14. Kyte, J. & Doolittle, R. F. (1982) *J. Mol. Biol.* **157**, 105–132.
15. Watson, M. E. (1984) *Nucleic Acids Res.* **12**, 5145–5164.
16. Hale, T. L., Schad, P. A. & Formal, S. B. (1983) *The Envelope in Tissue Invasion in Medical Microbiology* (Academic, London), Vol. 3, pp. 87–108.
17. Clerc, P., Baudry, B. & Sansonetti, P. J. (1986) *Ann. Microbiol. (Paris)* **134A**, 267–278.
18. Hopp, T. P. & Woods, K. R. (1981) *Proc. Natl. Acad. Sci. USA* **78**, 3824–3828.
19. Hall, M. N. & Silhavy, T. J. (1981) *Annu. Rev. Genet.* **15**, 91–142.
20. Hacker, J. & Hughes, C. (1985) *Curr. Top. Microbiol. Immunol.* **118**, 139–162.
21. Mooi, F. R. & DeGraaf, F. K. (1985) *Curr. Top. Microbiol. Immunol.* **118**, 119–138.
22. Mooi, F. R., Claasen, I., Bakker, D., Kuipers, H. & DeGraaf, F. K. (1986) *Nucleic Acids Res.* **14**, 2443–2458.
23. Isberg, R., Voorhis, D. L. & Falkow, S. (1987) *Cell* **50**, 769–778.
24. Jones, G. W. & Richardson, L. A. (1981) *J. Gen. Microbiol.* **127**, 361–370.
25. DeGraaf, F. K., Wientjes, F. B. & Klaasen, B. (1980) *Infect. Immun.* **27**, 216–221.
26. Bortolussi, R., Ferrieri, P. & Quie, P. G. (1983) *Infect Immun.* **39**, 1136–1141.
27. Yother, J., Chamness, T. W. & Goguen, J. D. (1986) *J. Bacteriol.* **165**, 443–447.
28. Straley, S. C. & Bowman, W. S. (1986) *Infect Immun.* **51**, 445–454.
29. Eilers, M. & Schatz, G. (1988) *Cell* **52**, 481–483.
30. Maurelli, A. T. & Sansonetti, P. J. (1988) *Proc. Natl. Acad. Sci. USA* **85**, 2820–2824.
31. Baga, M., Goransson, M., Normark, S. & Uhlin, B. E. (1988) *Cell* **52**, 197–206.